ACS OMEGA

Open Access

http://pubs.acs.org/journal/acsodf

Article

Mechanochemical Synthesis of Chromium(III) Complexes Containing Bidentate PN and Tridentate P-NH-P and P-NH-P′ Ligands

Tomilola J. Ajayi, Alan J. Lough, and Robert H. Morris*

Cite This: *ACS Omega* 2024, 9, 19690−19699

Read Online

ACCESS | Metrics & More | Article Recommendations | Supporting Information

ABSTRACT: Chromium(III) complexes bearing bidentate {$NH_2(CH_2)_2PPh_2$: PN, (*S*,*S*)-$[NH_2(CHPh)_2PPh_2]$: P′N} and tridentate $[Ph_2P(CH_2)_2N(H)(CH_2)_2PPh_2$: P-NH-P, (*S*,*S*)-$(iPr)_2PCH_2CH_2N(H)CH(Ph)CH(Ph)PPh_2$: P-NH-P′] ligands have been synthesized using a mechanochemical approach. The complexes {*cis*-$[Cr(PN)Cl_2]Cl$ (**1**), *cis*-$[Cr(P'N)Cl_2]Cl$ (**2**), *mer*-Cr(P-NH-P)Cl_3 (**3**), and *mer*-Cr(P-NH-P′)Cl_3 (**4**)} were obtained in high yield (95−97%) *via* the grinding of the respective ligands andthe solid Cr(III) ion precursor $[CrCl_3(THF)_3]$ with the aid of a pestle and mortar, followed by recrystallization in acetonitrile. The isolated complexes are high spin. A single-crystal X-ray diffraction study of **2** revealed a cationic chromium complex with two P′N ligands in a *cis* configuration with P′ *trans* to P′ with chloride as the counteranion. The X-ray study of **4** shows a neutral Cr(III) complex with the P-NH-P′ ligand in a *mer* configuration. The difference in molecular structures and bulkiness of the ligands influence the electronic, magnetic, and electrochemical properties of the complexes as exhibited by the bathochromic shifts in the electronic absorption peaks of the complexes and the relative increase in the magnetic moment of **3** (4.19 μ_β) and **4** (4.15 μ_β) above the spin only value (3.88 μ_β) for a d^3 electronic configuration. Complexes **1**−**4** were found to be inactive in the hydrogenation of an aldimine [(*E*)-1-(4-fluorophenyl)-*N*-phenylmethanimine] under a variety of activating conditions. The addition of magnesium and trimethylsilyl chloride in THF did cause hydrogenation at room temperature, but this occurred even in the absence of the chromium complex. The hydrogen in the amine product came from the THF solvent in this novel reaction, as determined by deuterium incorporation into the product when deuterated THF was used.

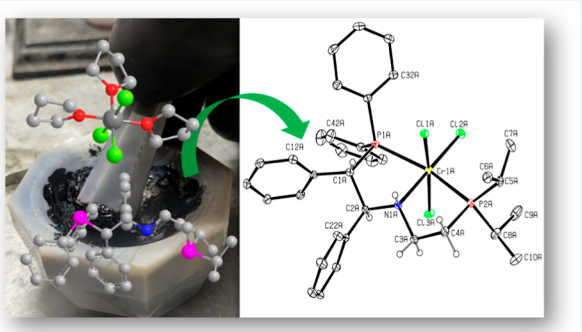

INTRODUCTION

The industrial demand for cheaper and less toxic alternative metals in the design of catalysts with higher efficiency and selectivity for essential fine chemicals in the flavor, perfumery, agricultural, and pharmaceutical industries is on the increase.[1−7] This has led to tremendous interest in the chemistry of first transition series elements which are more abundant and cheaper than the second and third transition series elements commonly given higher priority in catalytic design.[2,3,7−9] Among the first transition series elements, chromium has shown great potential in catalysis, especially when coordinated to aminophosphine (PN) and amino-diphosphine (PNP) ligands for the production of hex-1-ene and octa-1ene *via* trimerization and tetramerization of ethene.[10−15] The combination of hard (N) and soft (P) donors of these ligands is suitable to form stable complexes with Cr(III). The presence of hydrogen on the amino nitrogen, the varying of the substituents on the phosphine(s), and the introduction of asymmetric carbon provide endless possibilities in the synthesis of such metal complexes.[16−19] Complexes of chromium in several oxidation states have been synthesized including those of Cr(0) with a bidentate $PPh_2CH_2CH_2NH_2$ ligand,[20] Cr(III) with bidentate $Ph_2PNR'PPh_2$,[21] 2,6-R^1-4-R^2-$C_6H_2-N=CH-C_6H_4-2-PPh_2$[13] or $Ph_2PNMeCH_2CH_2C_5H_4N$[22] ligands, and Cr(II) with tridentate $[tBu_2PCHC_5H_3NCHPtBu_2]$[23] ligands, and their structures and catalytic properties were investigated. However, there is not a report on homochiral tridentate P-NH-P′ Cr complex with asymmetric carbon groups. Similarly, there are few reports of PN Cr complexes.[13,20] It is therefore not surprising that applications of such Cr complexes have not been given much consideration. Unlike Cr, chiral PN and unsymmetrical P-NH-P′ complexes of Ru,[24] Fe,[25−31] Mn,[32,33] and Ir[34] are known, and they have been explored in diverse applications.

The general routes adopted in the synthesis of these complexes often involve the use of solvents, which are often toxic and expensive. However, environmental safety concerns have given credence to the concept of green synthesis that

Received: March 2, 2024
Revised: April 2, 2024
Accepted: April 5, 2024
Published: April 16, 2024

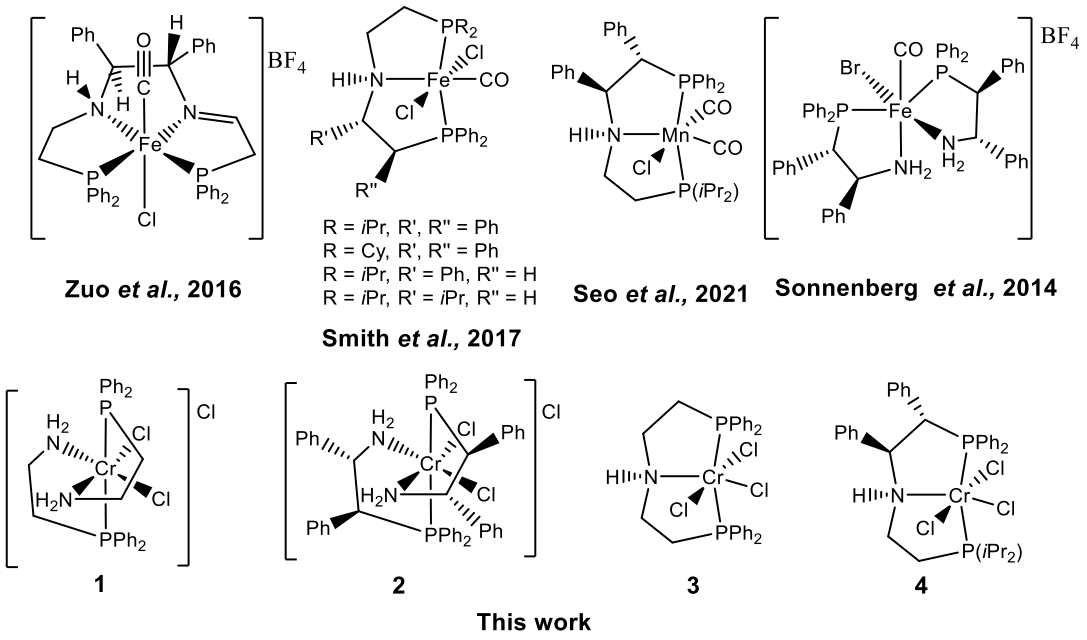

Figure 1. Representative of previously reported PNNP, P-NH-P′, and $(PN)_2$ complexes by our group and the new P-NH-P′ and PN chromium complexes in this work (see refs 17, 33, 38 and 39 for the structures shown).

minimizes or deliberately avoids the use of solvents. Mechanochemical techniques (dry grinding and liquid assisted grinding) are green routes to synthesize complexes without the use of solvent or with a few drops of solvent especially when the byproducts can be easily removed. This usually avoids the multiple purification and drying processes and also eliminates the generation of waste solvents.[20] These methods have been previously highlighted.[35] No reports of such a synthesis route have been adopted in the synthesis of metal complexes of chiral PN, P-NH-P, and P-NH-P′ ligands.

There are several protocols for the synthesis of chiral PN. However, the protocol developed by Guo *et al.*[36] provides a less complicated route with higher yield and purity. The unsymmetrical P-NH-P′ ligand can be derived from the chiral PN ligand *via* a condensation reaction with α-disubstituted phosphine acetaldehyde, as previously described by our group.[37] The tridentate P-NH-P′ pincer ligands are known to adopt different coordination modes around metal centers. In an octahedral coordinate geometry, the P-NH-P′ ligand can adopt a *mer* or *fac* coordination mode depending on the bulkiness of the substituents on the phosphines. The *mer* mode is thermodynamically more stable and more prevalent with bulky substituents.[30,32,38,39] Few examples of chromium complexes are known to adopt *fac* mode on the coordination of Cr(0) to tridentate $PPh_2CH_2CH_2N(C_2H_5)CH_2CH_2PPh_2$[40] and Cr(II) to $PPh_2CH_2Si(CH_3)_2NCH_2Si(CH_3)_2PPh_2$[41,42] ligand. There are several examples of chromium complexes that adopt *mer* mode with tridentate P-NH-P ethylene spacer groups,[14,43] PNP with phenylene backbone,[44,45] PNP disubstituted pyrrole backbone,[46] PNP disubstituted pyridine backbone,[47−52] PNP methylene-dimethylsilane backbone,[53,54] PNP disubstituted piperidine backbone,[55] PNP disubstituted triazine backbone,[56] and PNP substituted carbazole backbone.[57]

In the past, we have studied different Fe and Mn complexes of achiral and chiral PNNP[58−65] and unsymmetrical P-NH-P'[33,38,39,66,67] ligands, which have been demonstrated as efficient catalysts in asymmetric transfer hydrogenation and asymmetric pressure hydrogenation for the synthesis of chiral alcohols with high demand in the perfumery and pharmaceutical industries (Figure 1). However, a dearth of reports on the Cr complexes of these ligands prompted us to investigate the possible interactions and coordination modes that may exist between the Cr(III) ion and these ligands. Moreover, we also explore the mechanochemical technique as a green route for the synthesis of the complexes. Herein, we describe the synthesis, characterization, electrochemical properties, and crystal structures of Cr(III) complexes of chiral PN and unsymmetrical P-NH-P′ ligands.

RESULTS AND DISCUSSION

The preparations of the ligands [2-(diphenylphosphino)-ethylamine (PN), (1*S*,2*S*)-2-(diphenylphosphino)-1,2-diphenylethylamine (P'N), $Ph_2P(CH_2)_2N(H)(CH_2)_2PPh_2$ (P-NH-P), and (*S*,*S*)-$(iPr)_2PCH_2CH_2N(H)CH(Ph)CH(Ph)PPh_2$ (P-NH-P′)] have been previously reported by our group[38,39] and others,[14,43] and the details are provided in the Supporting Information. These pincer ligands were coordinated to Cr(III) using $CrCl_3(THF)_3$ as the Cr(III) precursor in an equimolar stoichiometric ratio *via* a mechanochemical synthesis. The synthesized complexes are listed in Figure 1. All attempts to synthesize $CrLCl_3(THF)$ (L: PN or P'N) by varying the stoichiometric ratios resulted in $[CrL_2Cl_2]^+$ (**1** and **2**). This reflects the strong affinity of the ligands for the Cr(III) ion. The complexes were dissolved in acetonitrile and left to crystallize at room temperature. Single crystals suitable for X-ray crystallographic study were obtained for complexes **2** and **4**. Complex **3** has been previously synthesized in THF, and the crystal structure was reported by McGuinness *et al.*[43] However, the use of a solvent was avoided in the method of synthesis adopted in this study. The similarity of the obtained product to the previously reported complex[43] shows that the same mechanism of interaction occurs between the metal salt and the ligands, with or without the use of solvent. This shows the viability of the adopted mechanochemical synthesis.[35,68,69] The report of McGuinness *et al.*[43] entails the crystal structure, mass

https://doi.org/10.1021/acsomega.4c02076
ACS Omega 2024, 9, 19690−19699

spectra, and elemental analyses of complex **3**. We provide more detailed characterization and electrochemical properties of complex **3** in this study for comparative analysis with the newly synthesized complexes **1**, **2**, and **4**.

Crystal Structure Analysis. The single-crystal X-ray diffraction study reveals that complex **2** crystallized in the orthorhombic space group $P2_12_12_1$ (Table S1). Two P'N ligands are coordinated to the Cr(III) *via* the N (amino) and P (phosphino) binding sites. The P binding sites occupy the axial position in a trans-conformation, while the two N sites are in the equatorial region in a cis-conformation (Figure 2).

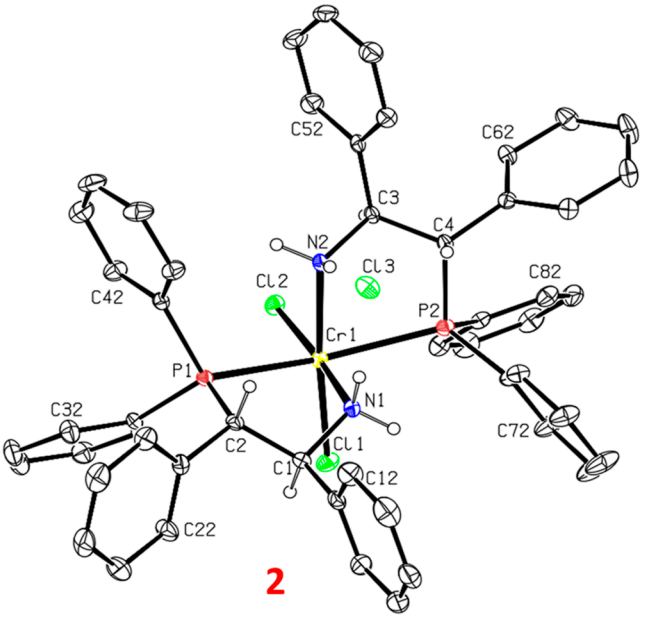

Figure 2. X-ray single-crystal structure of complex **2**. The hydrogen atoms of the phenyl groups have been omitted for the sake of clarity. The atomic symbols and the corresponding numbering of the elements in the structures are indicated for carbon (C), nitrogen (N), phosphorus (P), and chromium (Cr). Selected bond lengths (Å) and angles (deg) of complex **2**: Cr(1)−N(1) 2.086(3), Cr(1)−N(2) 2.104(3), Cr(1)−Cl(1) 2.3012(9), Cr(1)−Cl(2) 2.3053(9), Cr(1)−P(1) 2.4815(13), Cr(1)−P(2) 2.5030(13), N(1)−Cr(1)−N(2) 95.02(10), N(1)−Cr(1)−Cl(1) 86.32(8), N(2)−Cr(1)−Cl(1), 174.88(10), N(1)−Cr(1)−Cl(2) 175.57(10), N(2)−Cr(1)−Cl(2) 84.54(8), Cl(1)−Cr(1)−Cl(2) 94.50(3), P(1)−Cr(1)−P(2) 159.40(3), N(1)−Cr(1)−P(1) 79.52(10), N(2)−Cr(1)−P(1) 87.76(10), Cl(1)−Cr(1)−P(1) 97.34(5), Cl(2)−Cr(1)−P(1) 96.05(5), N(1)−Cr(1)−P(2) 85.96(10), N(2)−Cr(1)−P(2) 78.98(10), Cl(1)−Cr(1)−P(2) 96.21(5), and Cl(2)−Cr(1)−P(2) 98.27(5).

Similarly, two chlorides also coordinate to Cr(III) in a cis-conformation to complete the octahedral geometry. The coordinated P'N ligands form two five-membered rings with the Cr(III) center. The bond lengths around the Cr(III) center follow the covalent radii [P (1.11 Å), Cl (0.99 Å), and N (0.71 Å)] of the coordinated atoms in the order Cr−P > Cr−Cl > Cr−N. The bond angles 174.88° [N(2)−Cr−Cl(1)], 175.57° [N(1)−Cr−Cl(2)], and 159.40° [P(1)−Cr−P(2)] are less than 180 expected for an ideal octahedral complex, which reflect the distortion in complex **2** along its linear planes and also account for the twist of the P'N ligands as they coordinate to the Cr(III) center. Similar angular deviations from 90° are observed in the bond angles 79.52° [(N(1)−Cr−P(1)], 87.76° [N(2)−Cr−P(1)], and 97.34° [Cl(1)−Cr−P(1)] of the coordinated groups between the axial and equatorial planes, which also reflects the observed distortion in the geometry of the complex.

Unlike complex **2**, complex **4** with a tridentate P-NH-P′ ligand crystallized in the triclinic space group $P2_1$ (Table S1). The ligand coordinates *via* the P and N moieties of the phosphine and amino moieties in a meridional mode. The coordination of three Cl^- ions to the Cr(III) center completed the octahedral geometry. The Cl^- ions are dispersed along the Meridional plane transversely positioned to the P-NH-P′ ligand (Figure 3). This arrangement minimizes the geometric

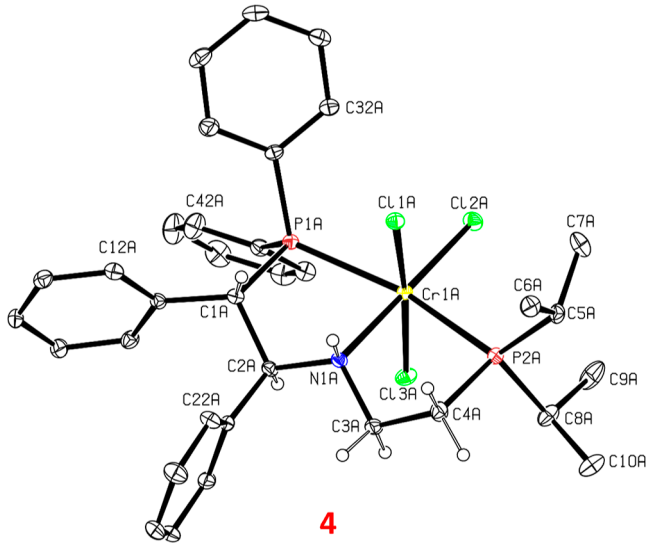

Figure 3. X-ray single-crystal structure of complex **4**. The hydrogen atoms of the phenyl and isopropyl groups have been omitted for the sake of clarity. The atomic symbols and the corresponding numbering of the elements in the structures are indicated for carbon (C), nitrogen (N), phosphorus (P), and chromium (Cr). Selected bond lengths (Å) and angles (deg) of complex **4**: Cr(1A)−N(1A) 2.136(2), Cr(1A)−Cl(2A) 2.3032(8), Cr(1A)−Cl(3A) 2.3205(8), Cr(1A)−Cl(1A) 2.3345(8), Cr(1A)−P(2A) 2.4734(9), Cr(1A)−P(1A) 2.5252(9), N(1A)−Cr(1A)−Cl(2A) 177.00(7), N(1A)−Cr(1A)−Cl(3A) 86.05(8), Cl(2A)−Cr(1A)−Cl(3A) 91.47(3), N-(1A)−Cr(1A)−Cl(1A) 84.80(8), Cl(2A)−Cr(1A)−Cl(1A) 97.72(3), Cl(3A)−Cr(1A)−Cl(1A) 170.67(3), N(1A)−Cr(1A)−P(2A) 82.18(7), Cl(2A)−Cr(1A)−P(2A) 99.49(3), Cl(3A)−Cr-(1A)−P(2A) 89.22(3), Cl(1A)−Cr(1A)−P(2A) 87.70(3), N(1A)−Cr(1A)−P(1A) 81.85(7), Cl(2A)−Cr(1A)−P(1A) 96.70(3), Cl-(3A)−Cr(1A)−P(1A) 95.06(3), Cl(1A)−Cr(1A)−P(1A) 85.49(3), and P(2A)−Cr(1A)−P(1A) 163.14(3).

constraints and enhances the thermodynamic stability of the complex in comparison to the facial mode.[70,71] The P-NH-P′ ligand forms two fused five-membered bicyclic rings with the Cr(III) center, with the C(2) and C(3) occupying an endo position to the N of the amino moiety.[32] The bond lengths Cr−Cl, Cr−N, and Cr−P are longer than those of complex **2** with the P'N ligand. This reflects the steric hindrance imposed by the bulkiness of the P-NH-P′,[33,38] which induces distortion in the octahedral geometry with elongated axial bond lengths 2.5252(9) Å [Cr−P(1)] and 2.4734(9) Å [Cr−P(2)] in comparison with the bond lengths along the equatorial plane. The bond angles also deviate from 90 and 180°, which also indicates distortion in the octahedral geometry of complex **4**. This can be attributed to the steric influence of the P-NH-P′

https://doi.org/10.1021/acsomega.4c02076
ACS Omega 2024, 9, 19690−19699

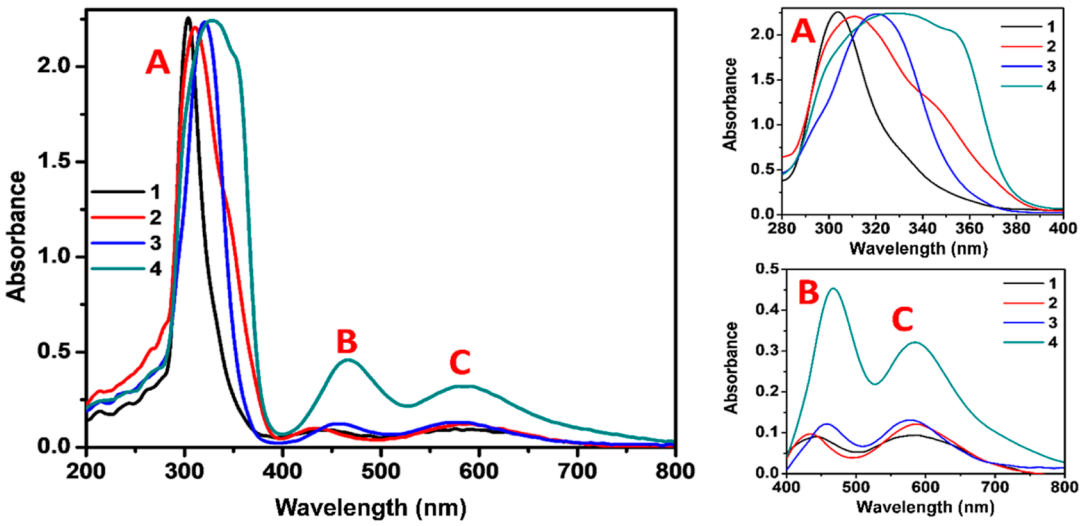

Figure 4. Electronic absorption spectra of complexes **1**−**4** in DMSO 1 mg/mL; [1.6 (**1**), 1.1 (**2**), 1.7 (**3**), and 1.5 (**4**) mM].

Table 1. Electronic Absorption Peak Wavelength (nm), the Corresponding Wavenumber (cm^{-1}), Molar Extinction Coefficient (ε; M^{-1} cm^{-1}), and Crystal Field Splitting Energy [Dq (cm^{-1})] of 1−4

	$\pi-\pi^*$	ε ($\pi-\pi^*$)	$^4A_{2g} \rightarrow {}^4T_{1g}$ (ν_2)	ε (ν_2)	$^4A_{2g} \rightarrow {}^4T_{2g}$ (ν_1)	ε (ν_1)	Dq
1	304 (32,895)	1415	439 (22,779)	60	584 (17,123)	55	1712
2	311 (32,154)	2022	436 (22,936)	90	588 (17,007)	111	1701
3	321 (31,153)	1316	459 (21,786)	72	578 (17,301)	78	1730
4	331 (30,211)	1496	468 (21,368)	301	586 (17,065)	214	1707
	354 (28,249) sh	1362					

ligand due to its bulkiness. Complex **4** has a strong structural similarity with previously reported complex **3**[43] as indicated by the closeness of the bond angles: P(1)−Cr−P(2) (**3**: 163.10°, **4**: 163.14°), N−Cr−Cl(2) (**3**: 176.74°, **4**: 177.00°), N−Cr−P(1) (**3**: 81.08°, **4**: 81.85°), and N−Cr−P(2) (**3**: 82.07°, **4**: 82.18°).

Electronic Absorption Spectra. The spectra of the complexes (**1**−**4**) in DMSO display an intense prominent absorption in the UV region (304−354 nm) (Figure 4A). This corresponds to intra-ligand transition which is strongly influenced by the nature of the ligand.[72] A considerable redshift and broadening were observed in the peak absorption wavelength on going from the cationic complexes **1** and **2** to the neutral complexes **3** and **4**. The order of the spin-allowed ligand field transitions characteristic of a Cr(III) complex with d^3 electronic configurations is $^4A_{2g} \rightarrow {}^4T_{2g}$ (ν_1) < $^4A_{2g} \rightarrow {}^4T_{1g}$ (F) (ν_2) < $^4A_{2g} \rightarrow {}^4T_{1g}$ (P) (ν_3).[73,74] We use these octahedral field symmetry labels in our work for comparison with assignments for literature complexes, even though our complexes are distorted from this ideal geometry. The low energy transition B in the region of 578−586 nm, the $^4A_{2g} \rightarrow {}^4T_{2g}$ (ν_1), has the energy of the ligand field splitting 10Dq (Table 1). Complexes **1** and **2** are thought to have similar *cis* geometries. However, the PN ligands in complex **1** have less hindered, more flexible backbones than the P'N ligands in complex **2**, and this causes a slightly larger splitting and stabilization of complex **1** (Dq = 1712 cm^{-1}) compared to complex **2** (Dq = 1701 cm^{-1}). Similarly, the more flexible PNP ligand causes the larger splitting in complex **3** (Dq = 1730 cm^{-1}) compared to complex **4** (Dq = 1707 cm^{-1}) with the more rigid PNP' ligand, even though the latter has a potentially more basic P*i*Pr$_2$ donor group. These Dq values are intermediate between those observed for $[CrCl_6]^{3-}$ (1360) and $[Cr(en)_3]^{3+}$ (2188)[75,76] as might be expected. The absorption peak B (Figure 4) in the region 439−468 nm can be attributed to $^4A_{2g} \rightarrow {}^4T_{1g}$ (F) ν_2 transition.[77,78] The spacing between the ν_1 and ν_2 transitions of the neutral complexes (4485 cm^{-1} for **3** and 4303 cm^{-1} for **4**) is smaller than that for the cationic complexes (5656 cm^{-1} for **1** and 5926 cm^{-1} for **2**). This spacing is even larger for $[Cr(OH_2)_6]^{3+}$ and $[Cr(NH_3)_6]^{3+}$ (>6000 cm^{-1}) due to an increase d electron repulsion as expressed by the Racah B parameter.[75] The transition of the highest energy [$^4A_{2g} \rightarrow {}^4T_{1g}$ (P)] is obscured by the more intense charge transfer transitions and would be expected in this case at approximately 40,000 cm^{-1} (12Dq + 15B + 9349) assuming the Racah parameter B is 680 cm^{-1} and the interaction energy between the two $^4T_{1g}$ states is 9349 cm^{-1} as determined from the position of ν_2.[79] The molar extinction coefficients (ε) observed for ν_1 (60−301 M^{-1} cm^{-1}) and ν_2 (55−214 M^{-1} cm^{-1}) (Table 1) are within the expected range for spin-allowed transitions.[74]

FTIR Vibrational Spectroscopy. The vibrational bands for ν(N−H) stretching in the region 3171−3298 cm^{-1} of the spectra of films of the complexes (**1**−**4**) indicate that the amino protons were retained after the coordination of the ligands to the Cr(III) center.[14,74] Hence, the amino ligands remained neutral, and the Cr(III) oxidation state was preserved. The vibrational bands in the region 400−500 cm^{-1} are characteristics of ν(Cr−Cl$^-$), which accounts for the chlorides in the coordination sphere.[74,77] It is intriguing to note that the influence of the difference in symmetric nature of the ligands becomes obvious as the primary amino protons in complex **2** display three vibrational bands (3201, 3242, and 3298 cm^{-1}) in contrast to complex **1**, where a single band (3173 cm^{-1}) is indicated for its primary amino protons. This difference is, however, not observed in complexes **3** and **4** with

https://doi.org/10.1021/acsomega.4c02076
ACS Omega 2024, 9, 19690−19699

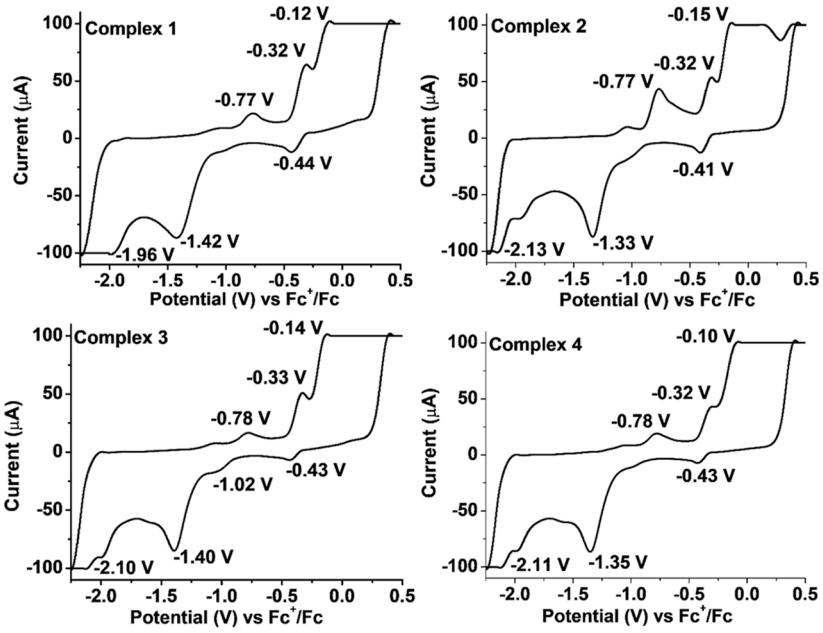

Figure 5. CVs of complexes **1**−**4** in 0.1 M [^{n}Bu$_4$N][BF$_4$]/DMF.

tridentate ligands, which contain secondary amino protons with vibrational bands at 3171 and 3286 cm^{-1}, respectively.

Magnetic Susceptibility and Electron Paramagnetic Resonance Spectroscopy. The effective magnetic moments (μ_{eff}) of complexes **1**−**4** were determined by the Evans' method.[80] The μ_{eff} for the complexes fall within the expected range of spin only magnetic moment ($\mu_{s.o}$ = 3.88 μ_β) for a d^3 electronic configuration.[80,81] The X-band electron paramagnetic resonance (EPR) spectra of complexes **1**−**4** as powders (see the Supporting Information) were obtained at room temperature and display the broad band characteristics of Cr(III) species with a d^3 electronic configuration.[82] The broad peaks hide any hyperfine couplings to the ^{31}P and ^{53}Cr nuclei.[21,83]

Electrochemical Study. The cyclic voltammogram (CV) of complex **1** (Figure 5) shows a complex series of redox events including Cr$^{III/II}$ and Cr$^{II/I}$ reduction processes with cathodic peak potentials (E_{pc}) at −0.44 and −1.42 V, and anodic peak potentials (E_{pa}) at −0.32 and −0.77 V. Reduction of substitution inert Cr^{III} produces labile Cr^{II}, resulting in irreversible electrochemical behavior. The E_{pa} at −0.12 V indicates an irreversible oxidation of Cl$^-$ with a surge in current as the product of the oxidation (Cl_2 gas) desorbed from the surface of the electrode.[84,85] The redox activity associated with Cl$^-$ is equally observed by measuring the CV of tetrabutyl ammonium chloride (TBA$^+$ Cl$^-$) in DMF and MeCN, where a similar increase in current is indicated in the CVs at −0.18 and −0.09 V in DMF and MeCN, respectively (Figure S6). The high potential suggests the substitution of dissociated Cl$^-$ with a solvent molecule (DMF) from reduced chromium species (eqs 1, 2).

$$[CrCl_2(PN)_2]^+ + e^- \rightleftharpoons [CrCl_2(PN)_2] \quad (1)$$

$$[CrCl_2(PN)_2] + \text{solvent} \rightleftharpoons [CrCl(\text{solvent})(PN)_2]^+ + Cl^- \quad (2)$$

Similarly, an irreversible reduction at E_{pc} of −1.96 V can be attributed to the substitution of the PN ligand with DMF.[86,87] The CV of complex **2** also shows a two-step electron transfer processes with E_{pc} at −0.41 and −1.33 V and corresponding E_{pa} at −0.32 and −0.77 V. The rapid increase in current in the region where E > −0.15 V again suggests the contribution of the irreversible Cl$^-$ ion oxidation/substitution with DMF. The CVs of the complexes with tridentate ligands (**3** and **4**) also reveal a two-step electron transfer characteristic of Cr ion. The influence of the Cl$^-$ ion oxidation significantly increased the current in the region where E > −0.10 V (eq 3), and the involvement/substitution of the PNP and PNP' ligands can be attributed to the E_{pc} at −2.10 and −2.11 V in the CV of complex **3** and **4**, respectively.

$$[CrCl_3(PNP)]^- + \text{solvent} \rightleftharpoons [CrCl_2(\text{solvent})(PNP)] + Cl^- \quad (3)$$

The likely substitution of the Cl$^-$ and the pincer ligands with solvent molecules in the electrochemical process is further investigated by replacing DMF with MeCN.[73] MeCN significantly shifts the redox potentials in the electrochemical process, especially for the potentials associated with the substitution of the Cl$^-$ and pincer ligands (Figure S7).

Lack of Catalytic Activity of Complexes 1−4 in Hydrogenation Reactions. The catalytic activity of the chromium complexes (**1**−**4**) was investigated in the hydrogenation of the aldimine [(*E*)-1-(4-fluorophenyl)-*N*-phenylmethanimine] to the amine [*N*-(4-fluorobenzyl)aniline] using molecular H_2 under 25 bar in THF at 60 °C with a 5 mol % catalytic loading. The reaction was monitored by ^{19}F NMR spectroscopy. Complexes **1**−**4** showed no observable activity. Further catalytic investigations were carried out using complexes **1**−**4** (1 mol %) in the asymmetric transfer hydrogenation of diphenylphosphinoyl imines to their respective amines analogues using KO^{t}Bu (8 mol %) as a base and 2-PrOH as a solvent and as a reducing agent at 30 °C.[62,88,89] After 24 h, no conversion was noted using ^{31}P NMR spectroscopy to monitor the reaction. We envisaged the possible activation of the complexes by the generation of their corresponding hydrides using LiHBEt$_3$ in THF at −30 to 28 °C to induce their catalytic activity in transfer hydro-

https://doi.org/10.1021/acsomega.4c02076
ACS Omega 2024, 9, 19690−19699

Table 2. Catalytic Study of Hydrogenation of an Imine (0.1 M) to an Amine

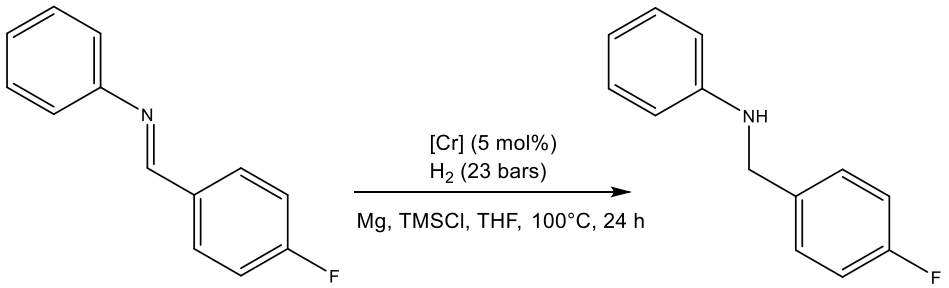

entry	[Cr]	Mg (equiv)	TMSCl (equiv)	yield (%)
1	**1**	2	0.5	98
2	**2**	2	0.5	100
3	**3**	2	0.5	96
4	**4**	2	0.5	97
5		2	0.5	99
6[a]				32
7[b]				33
8[c]		2	0.5	99
9[c,d]		2	0.5	90
10[c,d,e]		2	0.5	20

[a]Grignard reagent ($PhCH_2MgCl$). [b]Activated Mg. [c]Under Ar. [d]22 °C. [e]THF-D_8 was used as the solvent.

genation.[38,90] The formation of hydrides was not successful. We also attempted to aid the hydride formation of the complexes by first generating the triflate analogues of the complexes **1**−**4** but the complexes showed no reaction in the presence of AgOTf in toluene. On the basis of these negative results, we did not proceed further on investigating the complexes as catalysts in transfer hydrogenation.

Following a recent report on the chromium complexes of cyclic (alkyl)(amino) carbene (CAAC)-catalyzed hydrogenation of alkynes for the selective generation of *E*- and *Z*- olefins with high yield in the presence of Mg and trimethylsilyl chloride (TMSCl),[91] we further investigated the possibility that our complexes **1**−**4** are catalysts for the conversion of imine [(*E*)-1-(4-fluorophenyl)-*N*-phenylmethanimine] to amine [*N*-(4-fluorobenzyl)aniline] using H_2. However, our preliminary investigation showed that the hydrogenation to the amine proceeded in the presence of Mg and TMSCl with or without our complexes as catalysts (Table 2, entries 1−5). We wondered whether the hydrogenation proceeded *via* the *in situ* generation of a Grignard-like reagent from Mg and TMSCl. However, when only the Grignard reagent ($PhCH_2MgBr$) (entry 6) or activated Mg (entry 7) was used under H_2 in the absence of a chromium complex, lower conversion to the amine was observed. Furthermore, when we excluded H_2 (entry 8) and conducted the reaction under Ar at room temperature (entry 9), the hydrogenation still proceeded. This implicates the solvent (THF) as being the hydrogen source. We confirmed this hypothesis by conducting two separate experiments. In the first, the dideuterated amine $PhNDCDHC_6H_4F$ was generated by the reaction of the imine with $NaBD_4$ in CD_3OD in order to obtain its ^{19}F NMR and mass spectrum. Then, deuterated THF-D_8 (entry 10) was used as the solvent in the Mg/TMSCl reaction under the same conditions as in entry 9 but with a longer duration (48 h). The mass spectrum of the isolated crude amine product was consistent with partial conversion to the deuterated amine $PhNDCDHC_6H_4F$. However, the conversion was less than that of entry 9, presumably because of the significant kinetic isotope effect of breaking the carbon-deuterium bond of the THF-D_8 [BDE(C−H) 92 kcal/mol[92]. Thus, we suggest that the hydrogenation proceeds by magnesium reduction of the imine or TMS-iminium chloride with hydrogen atom abstraction from the THF. This side reaction was not reported for the Cr(CAAC) complexes that showed catalytic activity and selectivity in the hydrogenation of alkynes in the presence of Mg/TMSCl in THF.[91]

CONCLUSIONS

We have demonstrated the preparation of new Cr(III) complexes in high-yield (95−97%) with a solventless mechanochemical approach and studied the electronic, magnetic, and electrochemical properties of these complexes. The structural analysis revealed that the bidentate P'N ligands form a *cis* complex with *trans* Cr−P bonds. The P-NH-P′ ligand coordinates in a *mer* arrangement about the Cr(III) center with three *mer* Cl^- ions. In the case of complex **1**, no suitable crystals were obtained for the X-ray diffraction study. However, we envisage that it will adopt a structural configuration similar to that of complex **2** based on similarity in properties just as complex **4** shows strong structural resemblance to the previously reported complex **3**. The structural differences in the ligands induce variations in the electronic, magnetic, and electrochemical properties of the complexes, which influence their stability. The only conditions discovered for the hydrogenation of an aldimine did not involve the chromium complexes but instead involved the novel reduction of the imine by a Mg/TMSCl mixture under Ar at room temperature with hydrogen abstraction from the THF solvent.

EXPERIMENTAL SECTION

General Experimental Details. All the procedures and modifications reported in this work were conducted under a N_2 of Ar atmosphere using standard Schlenk line and glovebox facilities, unless otherwise stated. The reagents were used as received from Sigma-Aldrich, Alfa Aesar, and ACROS

https://doi.org/10.1021/acsomega.4c02076
ACS Omega 2024, 9, 19690−19699

Organics. All solvents were predegassed and dried based on standard procedures before the commencement of each experiment. The ^{1}H (500 MHz) NMR spectra were recorded on an Agilent DD2 500 MHz. The FTIR spectra were acquired on a Bruker Alpha spectrometer equipped with an ATR platinum-diamond attachment. X-ray crystallographic data for **2** and **4** were collected on a Bruker Kappa APEX-DUO diffractometer equipped with a PHOTON II CMOS detector and were measured using a combination of ϕ scans and ω scans. The data were processed using APEX3 and SAINT. Mass spectra were obtained with a JEOL AccuTOF Plus 4G equipped with a direct analysis in real time ion source. The absorption spectra were measured by using DMSO solutions of the complexes (**1**−**4**). For the Evans' method,[80] the NMR frequency was 500 MHz, and the reference solvent used for **1** was C_4H_8O/C_4D_8O, while CH_3CN/CD_3CN was used for **2**−**4**. The X-band EPR spectra were obtained by using a Bruker CW X-band ECS-EMXplus EPR spectrometer at 9.5 GHz. The electrochemical study was conducted using a three-electrode setup with a platinum wire as a working electrode, a tungsten auxiliary electrode, and a Ag/AgCl reference electrode. The electrolyte was a DMF solution with 0.1 M $[^nBu_4N][BF_4]$. All potentials were referenced to the ferrocenium/ferrocene (Fc^+/Fc) couple (0.72 V versus the standard hydrogen electrode, SHE).[67] All characterizations were conducted using powder products of the complexes, except for the X-ray diffraction studies using crystals obtained from MeCN.

Mechanochemical Synthesis. *[Cr(PN)$_2$Cl$_2$]Cl (**1**).* Purple $CrCl_3(THF)_3$ (0.24 g, 0.65 mmol) and white PN (0.30 g, 1.3 mmol) were ground with a pestle and mortar in a glovebox for 5 min to a dark blue powder and left overnight at room temperature. A solid product was obtained. Yield: 97% (0.39 g, 0.63 mmol). HRMS: calcd for $C_{28}H_{35}Cl_3CrN_2P_2$, 619.90 ($[M]^+$); found, (ESI^+): 619.06. EA: % Anal. Calcd (found) for $C_{28}H_{35}Cl_3CrN_2P_2$: 619.90 g/mol: C, 54.25 (54.19); H, 5.69 (5.62); N, 4.52 (4.49). FT-IR (ATR, ν/cm^{-1}): 3173 (m, NH_2), 3053, (m, CH), 2949 (m, CH), 2924 (m, CH), 2870 (m, CH), 459 (s, Cr−Cl), 437 (s, Cr−Cl). μ_{eff}: 3.31 μ_β.

*[Cr(P′N)$_2$Cl$_2$]Cl (**2**).* $CrCl_3(THF)_3$ (0.24 g, 0.65 mmol) and white P′N (0.50 g, 1.3 mmol) were ground with a pestle and mortar in a glovebox for 5 min to a dark blue powder and left overnight at room temperature. A solid product was obtained, which was dissolved in acetonitrile and left to recrystallize at room temperature for use in the X-ray diffraction study. Yield: 95% (0.57 g, 0.62 mmol). HRMS: calcd for $C_{52}H_{51}Cl_3CrN_2P_2$, 922.20 ($[M]^+$); found, (ESI^+): 922.01. EA: % Anal. Calcd (found) for $C_{52}H_{51}Cl_3CrN_2P_2$: 922.20 g/mol: C, 67.57 (67.54); H, 5.56 (5.57); N, 3.03 (3.07). FT-IR (ATR, ν/cm^{-1}): 3298 (w, NH_2), 3242 (w, NH_2), 3201 (w, NH_2), 3062, (w, CH), 2980 (w, CH), 459 (m, Cr−Cl), 432 (m, Cr−Cl). μ_{eff}: 3.23 μ_β.

*[Cr(P-NH-P)Cl$_3$] (**3**).* $CrCl_3(THF)_3$ (0.48 g, 1.3 mmol) and white P-NH-P (0.57 g, 1.3 mmol) were ground with a pestle and mortar in a glovebox for 5 min to a dark blue powder and left overnight at room temperature. A solid product was obtained. Yield: 96% (0.75 g, 1.25 mmol). HRMS: calcd for $C_{28}H_{29}Cl_3CrNP_2$, 598.02 ($[M]^+$); found, (ESI^+): 598.04. EA: % Anal. Calcd (found) for with Mol wt for $C_{28}H_{29}Cl_3CrNP_2$: 598.02 g/mol: C, 56.07 (56.12); H, 4.87 (4.9); N, 2.34 (2.36). FT-IR (ATR, ν/cm^{-1}): 3171 (m, NH), 3053 (w, CH), 2950 (w, CH), 2924, (w, CH), 2870 (w, CH), 458 (m, Cr−Cl), 436 (m, Cr−Cl). μ_{eff} 4.19 μ_β.

*[Cr(P-NH-P′)Cl$_3$] (**4**).* $CrCl_3(THF)_3$ (0.48 g, 1.3 mmol) and P-NH-P′ (0.77 g, 1.3 mmol) were mixed with a pestle and mortar in a glovebox for 5 min and left overnight at room temperature. A dark blue solid product was obtained. Crystals suitable for X-ray diffraction were obtained by recrystallization from acetonitrile at room temperature. Yield: 95% (0.85 g, 1.24 mmol). HRMS: calcd for $C_{34}H_{41}Cl_3CrNP_2$, 647.15 ($[M - Cl]^+$); found, (ESI^+): 647.21. EA: % Anal. Calcd for $C_{34}H_{41}Cl_3CrNP_2$: 683.97 g/mol: C, 59.41 (59.47); H, 6.26 (6.26); N, 1.96 (1.95). FT-IR (ATR, ν/cm^{-1}): 3286 (m, NH), 3056 (w, CH), 3030 (w, CH), 2918, 497 (m, Cr−Cl), 477 (m, Cr−Cl), 456 (w, Cr−Cl), 433 (w, Cr−Cl). μ_{eff}: 4.15 μ_β.

General Procedure for Catalytic Study. The catalytic study was conducted based on a modified procedure.[91] Briefly, the imine (0.2 mmol, 40 mg), the synthesized complex (5 mol %), Mg (10 mg), TMSCl (13 μL), and THF (2 mL) were stirred continuously in a vial under an argon atmosphere. The reaction mixture was transferred to a 50 mL stainless steel Parr hydrogenation reactor at constant temperatures (aided with an oil bath) and pressures (23 atm of $H_{2(g)}$) with continuous stirring. The crude product was extracted in ethyl acetate (3 × 5 mL) after quenching the reaction with aqueous HCl (1 M, 2 mL). This was followed by drying the product in ethyl acetate over anhydrous Na_2SO_4 before removing the solvent in vacuo. The conversion was determined from the ^{19}F NMR signal of the crude product (−115.6 ppm, 400 MHz, $CDCl_3$) relative to that of the starting imine (−108.02 ppm, 400 MHz, $CDCl_3$).

■ ASSOCIATED CONTENT

Supporting Information

The Supporting Information is available free of charge at https://pubs.acs.org/doi/10.1021/acsomega.4c02076.

Synthesis of the ligands and complexes, FTIR spectra, selected X-ray diffraction information, CVs, synthesis of the imine, spectra corresponding to the entries of Table 2, and synthesis of the dideuterated amine (PDF)

Crystal structure data for complex **2** (CIF)

Crystal structure data for complex **4** (CIF)

Accession Codes

CCDC 2293698−2293699 contain the supplementary crystallographic data for this paper. These data can be obtained free of charge via www.ccdc.cam.ac.uk/data_request/cif, or by emailing data_request@ccdc.cam.ac.uk, or by contacting the Cambridge Crystallographic Data Centre, 12 Union Road, Cambridge CB2 1EZ, UK; fax: +44 1223 336033.

■ AUTHOR INFORMATION

Corresponding Author

Robert H. Morris − *Department of Chemistry, University of Toronto, Toronto M5S3H6 Ontario, Canada;* orcid.org/0000-0002-7574-9388; Email: rmorris@chem.utoronto.ca

Authors

Tomilola J. Ajayi − *Department of Chemistry, University of Toronto, Toronto M5S3H6 Ontario, Canada*

Alan J. Lough − *Department of Chemistry, University of Toronto, Toronto M5S3H6 Ontario, Canada;* orcid.org/0000-0001-6012-0379

Complete contact information is available at: https://pubs.acs.org/10.1021/acsomega.4c02076

https://doi.org/10.1021/acsomega.4c02076
ACS Omega 2024, 9, 19690−19699

Notes

The authors declare no competing financial interest.

■ ACKNOWLEDGMENTS

T.J.A. thanks the South African government for a Fellowship. R.H.M. thanks the NSERC (Canada) for a Discovery grant.

■ REFERENCES

(1) Morris, R. H. Asymmetric hydrogenation, transfer hydrogenation and hydrosilylation of ketones catalyzed by iron complexes. *Chem. Soc. Rev.* **2009**, *38*, 2282−2291.
(2) Bullock, R. M.; Chen, J. G.; Gagliardi, L.; Chirik, P. J.; Farha, O. K.; Hendon, C. H.; Jones, C. W.; Keith, J. A.; Klosin, J.; Minteer, S. D.; et al. Using nature's blueprint to expand catalysis with earth-abundant metals. *Science* **2020**, *369*, No. eabc3183.
(3) Seo, C. S.; Morris, R. H. Catalytic homogeneous asymmetric hydrogenation: successes and opportunities. *Organometallics* **2019**, *38*, 47−65.
(4) Manßen, M.; Scott, S. S.; Deng, D.; Zheng, C. H.; Schafer, L. L. Accessing secondary amine containing fine chemicals and polymers with an earth-abundant hydroaminoalkylation catalyst. *Green Chem.* **2023**, *25*, 2629−2639.
(5) Wen, J.; Wang, F.; Zhang, X. Asymmetric hydrogenation catalyzed by first-row transition metal complexes. *Chem. Soc. Rev.* **2021**, *50*, 3211−3237.
(6) Rana, S.; Biswas, J. P.; Paul, S.; Paik, A.; Maiti, D. Organic synthesis with the most abundant transition metal-iron: from rust to multitasking catalysts. *Chem. Soc. Rev.* **2021**, *50*, 243−472.
(7) Liu, Y.; You, T.; Wang, H.-X.; Tang, Z.; Zhou, C.-Y.; Che, C.-M. Iron-and cobalt-catalyzed C(sp 3)-H bond functionalization reactions and their application in organic synthesis. *Chem. Soc. Rev.* **2020**, *49*, 5310−5358.
(8) Lu, C. C.; Bill, E.; Weyhermüller, T.; Bothe, E.; Wieghardt, K. Neutral bis (α-iminopyridine) Metal complexes of the first-row transition ions (Cr, Mn, Fe, Co, Ni, Zn) and their monocationic analogues: mixed valency involving a redox noninnocent ligand system. *J. Am. Chem. Soc.* **2008**, *130*, 3181−3197.
(9) Yang, P.; Xu, H.; Zhou, J. Nickel-Catalyzed asymmetric transfer hydrogenation of olefins for the synthesis of α-and β-Amino acids. *Angew. Chem., Int. Ed.* **2014**, *53*, 12210−12213.
(10) Nifant'ev, I. E.; Vinogradov, A. A.; Vinogradov, A. A.; Roznyatovsky, V. A.; Grishin, Y. K.; Ivanyuk, A. V.; Sedov, I. V.; Churakov, A. V.; Ivchenko, P. V. 5, 6-Dihydrodibenzo [c, e] [1, 2] azaphosphinine-based PNP ligands, Cr (0) coordination, and Cr(III) precatalysts for ethylene oligomerization. *Organometallics* **2018**, *37*, 2660−2664.
(11) Blann, K.; Bollmann, A.; de Bod, H.; Dixon, J. T.; Killian, E.; Nongodlwana, P.; Maumela, M. C.; Maumela, H.; McConnell, A. E.; Morgan, D. H. Ethylene tetramerisation: subtle effects exhibited by N-substituted diphosphinoamine ligands. *J. Catal.* **2007**, *249*, 244−249.
(12) Suttil, J. A.; Wasserscheid, P.; McGuinness, D. S.; Gardiner, M. G.; Evans, S. J. A Survey of pendant donor-functionalised (N, O) phosphine ligands for Cr-catalysed ethylene tri-and tetramerisation. *Catal. Sci. Technol.* **2014**, *4*, 2574−2588.
(13) Zheng, Q.; Zheng, D.; Han, B.; Liu, S.; Li, Z. Chromium complexes supported by the bidentate PN ligands: synthesis, characterization and application for ethylene polymerization. *Dalton Trans.* **2018**, *47*, 13459−13465.
(14) McGuinness, D. S.; Brown, D. B.; Tooze, R. P.; Hess, F. M.; Dixon, J. T.; Slawin, A. M. Ethylene trimerization with Cr- PNP and Cr- SNS complexes: effect of ligand structure, metal oxidation state, and role of activator on catalysis. *Organometallics* **2006**, *25*, 3605−3610.
(15) Peitz, S.; Peulecke, N.; Müller, B. H.; Spannenberg, A.; Drexler, H.-J.; Rosenthal, U.; Al-Hazmi, M. H.; Al-Eidan, K. E.; Wöhl, A.; Müller, W. Heterobimetallic Al- Cl- Cr intermediates with relevance to the selective catalytic ethene trimerization systems consisting of $CrCl_3$ (THF) 3, the aminophosphorus ligands $Ph_2PN(R)P(Ph)N$-(R)H, and triethylaluminum. *Organometallics* **2011**, *30*, 2364−2370.
(16) Zuo, W.; Tauer, S.; Prokopchuk, D. E.; Morris, R. H. Iron catalysts containing amine (imine) diphosphine P-NH-NP ligands catalyze both the asymmetric hydrogenation and asymmetric transfer hydrogenation of ketones. *Organometallics* **2014**, *33*, 5791−5801.
(17) Zuo, W.; Prokopchuk, D. E.; Lough, A. J.; Morris, R. H. Details of the mechanism of the asymmetric transfer hydrogenation of acetophenone using the amine (imine) diphosphine iron precatalyst: the base effect and the enantiodetermining step. *ACS Catal.* **2016**, *6*, 301−314.
(18) Younus, H. A.; Su, W.; Ahmad, N.; Chen, S.; Verpoort, F. Ruthenium pincer complexes: synthesis and catalytic applications. *Adv. Synth. Catal.* **2015**, *357*, 283−330.
(19) Wang, H.; Wen, J.; Zhang, X. Chiral tridentate ligands in transition metal-catalyzed asymmetric hydrogenation. *Chem. Rev.* **2021**, *121*, 7530−7567.
(20) Vielhaber, T.; Faust, K.; Topf, C. Group 6 metal carbonyl complexes supported by a bidentate PN ligand: syntheses, characterization, and catalytic hydrogenation activity. *Organometallics* **2020**, *39*, 4535−4543.
(21) Venderbosch, B.; Wolzak, L. A.; Oudsen, J.-P. H.; de Bruin, B.; Korstanje, T. J.; Tromp, M. role of the ligand and activator in selective Cr-PNP ethene tri-and tetramerization catalysts-a spectroscopic study. *Catal. Sci. Technol.* **2020**, *10*, 6212−6222.
(22) Shaikh, Y.; Gurnham, J.; Albahily, K.; Gambarotta, S.; Korobkov, I. Aminophosphine-based chromium catalysts for selective ethylene tetramerization. *Organometallics* **2012**, *31*, 7427−7433.
(23) Simler, T.; Frison, G.; Braunstein, P.; Danopoulos, A. A. Direct synthesis of doubly deprotonated, dearomatised lutidine PNP Cr and Zr pincer complexes based on isolated K and Li ligand transfer reagents. *Dalton Trans.* **2016**, *45*, 2800−2804.
(24) Chiu, P. L.; Lee, H. M. Chemistry of the PCNHCP ligand: silver and ruthenium complexes, facial/meridional coordination, and catalytic transfer hydrogenation. *Organometallics* **2005**, *24*, 1692−1702.
(25) Mikhailine, A.; Lough, A. J.; Morris, R. H. Efficient asymmetric transfer hydrogenation of ketones catalyzed by an iron complex containing a P- N- N- P tetradentate ligand formed by template synthesis. *J. Am. Chem. Soc.* **2009**, *131*, 1394−1395.
(26) Mikhailine, A. A.; Maishan, M. I.; Lough, A. J.; Morris, R. H. The mechanism of efficient asymmetric transfer hydrogenation of acetophenone using an iron(II) complex containing an (S, S)-Ph_2PCH_2CH = NCHPhCHPhN = $CHCH_2PPh_2$ ligand: partial ligand reduction is the key. *J. Am. Chem. Soc.* **2012**, *134*, 12266−12280.
(27) Sonnenberg, J. F.; Coombs, N.; Dube, P. A.; Morris, R. H. Iron nanoparticles catalyzing the asymmetric transfer hydrogenation of ketones. *J. Am. Chem. Soc.* **2012**, *134*, 5893−5899.
(28) Lagaditis, P. O.; Lough, A. J.; Morris, R. H. Iron complexes for the catalytic transfer hydrogenation of acetophenone: steric and electronic effects imposed by alkyl substituents at Phosphorus. *Inorg. Chem.* **2010**, *49*, 10057−10066.
(29) Meyer, N.; Lough, A. J.; Morris, R. H. Iron(II) complexes for the efficient catalytic asymmetric transfer hydrogenation of ketones. *Chem.—Eur. J.* **2009**, *15*, 5605−5610.
(30) Huber, R.; Passera, A.; Gubler, E.; Mezzetti, A. P-Stereogenic PN (H) P iron(II) catalysts for the asymmetric hydrogenation of ketones: the importance of non-covalent interactions in rational ligand design by computation. *Adv. Synth. Catal.* **2018**, *360*, 2900−2913.
(31) Uchiike, C.; Ouchi, M.; Ando, T.; Kamigaito, M.; Sawamoto, M. Evolution of iron catalysts for effective living radical polymerization: P-N chelate ligand for enhancement of catalytic performances. *J. Polym. Sci.* **2008**, *46*, 6819−6827.
(32) Passera, A.; Mezzetti, A. Mn(I) and Fe(II)/PN(H)P catalysts for the hydrogenation of ketones: a comparison by experiment and calculation. *Adv. Syn. Catal.* **2019**, *361*, 4691−4706.
(33) Seo, C. S.; Tsui, B. T.; Gradiski, M. V.; Smith, S. A.; Morris, R. H. Enantioselective direct, base-free hydrogenation of ketones by a

https://doi.org/10.1021/acsomega.4c02076
ACS Omega 2024, 9, 19690−19699

manganese amido complex of a homochiral, unsymmetrical P-N-P′ ligand. *Catal. Sci. Technol.* **2021**, *11*, 3153−3163.
(34) Wang, H.; Zhang, Y.; Yang, T.; Guo, X.; Gong, Q.; Wen, J.; Zhang, X. Chiral electron-rich PNP ligand with a phospholane motif: structural features and application in asymmetric hydrogenation. *Org. Lett.* **2020**, *22*, 8796−8801.
(35) DeGroot, H. P.; Hanusa, T. P. Solvate-assisted grinding: metal solvates as solvent sources in mechanochemically driven organometallic reactions. *Organometallics* **2021**, *40*, 3516−3525.
(36) Guo, R.; Lu, S.; Chen, X.; Tsang, C.-W.; Jia, W.; Sui-Seng, C.; Amoroso, D.; Abdur-Rashid, K. Synthesis of chiral aminophosphines from chiral aminoalcohols via cyclic sulfamidates. *J. Org. Chem.* **2010**, *75*, 937−940.
(37) Mikhailine, A. A.; Lagaditis, P. O.; Sues, P. E.; Lough, A. J.; Morris, R. H. New cyclic phosphonium salts derived from the reaction of phosphine-aldehydes with acid. *J. Organomet. Chem.* **2010**, *695*, 1824−1830.
(38) Smith, S. A.; Lagaditis, P. O.; Lüpke, A.; Lough, A. J.; Morris, R. H. Unsymmetrical iron P-NH-P′ catalysts for the asymmetric pressure hydrogenation of aryl ketones. *Chem.—Eur. J.* **2017**, *23*, 7212−7216.
(39) Sonnenberg, J. F.; Lough, A. J.; Morris, R. H. Synthesis of iron PNP′ and P-NH-P′ asymmetric hydrogenation catalysts. *Organometallics* **2014**, *33*, 6452−6465.
(40) Cotton, F. A.; LaPrade, M. D. Crystal and molecular structures of [N,N-bis(2-diphenylphosphinoethyl) ethylamine] tricarbonylchromium. *J. Am. Chem. Soc.* **1969**, *91*, 7000−7005.
(41) Fryzuk, M. D.; Leznoff, D. B.; Rettig, S. J.; Thompson, R. C. Magnetic exchange in dinuclear chromium(II) complexes: effect of bridging chlorides and bridging hydrides in antiferromagnetic coupling. *Inorg. Chem.* **1994**, *33*, 5528−5534.
(42) Fryzuk, M. D.; Leznoff, D. B.; Rettig, S. J. Synthesis and structure of even-electron paramagnetic chromium(II) complexes. *Organometallics* **1995**, *14*, 5193−5202.
(43) McGuinness, D. S.; Wasserscheid, P.; Keim, W.; Hu, C.; Englert, U.; Dixon, J. T.; Grove, C. novel Cr-PNP complexes as catalysts for the trimerisation of ethylene. *Chem. Commun.* **2003**, 334−335.
(44) Bluhm, M. E.; Walter, O.; Döring, M. Chromium imine and amine complexes as homogeneous catalysts for the trimerisation and polymerisation of ethylene. *J. Organomet. Chem.* **2005**, *690*, 713−721.
(45) Liu, Q.; Gao, R.; Hou, J.; Sun, W. Tridentate P̂NP Chromium Complexes: Synthesis, Character-ization and Their Ethylene Oligomerization and Polymerization. *Chin. J. Org. Chem.* **2013**, *33*, 808.
(46) Kuriyama, S.; Arashiba, K.; Nakajima, K.; Tanaka, H.; Yoshizawa, K.; Nishibayashi, Y. Azaferrocene-based PNP-Type pincer ligand: synthesis of molybdenum, chromium, and iron complexes and reactivity toward nitrogen fixation. *Eur. J. Inorg. Chem.* **2016**, *2016*, 4856−4861.
(47) Alzamly, A.; Gambarotta, S.; Korobkov, I. Polymer-free ethylene oligomerization using a pyridine-based pincer PNP-type of ligand. *Organometallics* **2013**, *32*, 7204−7212.
(48) Alzamly, A.; Gambarotta, S.; Korobkov, I. Reactivity with alkylaluminum of a chromium complex of a pyridine-containing PNP ligand: redox N-P bond cleavage. *Organometallics* **2014**, *33*, 1602−1607.
(49) Mastalir, M.; Glatz, M.; Stöger, B.; Weil, M.; Pittenauer, E.; Allmaier, G.; Kirchner, K. Synthesis, characterization and reactivity of vanadium, chromium, and manganese PNP pincer complexes. *Inorg. Chim. Acta* **2017**, *455*, 707−714.
(50) Gong, D.; Liu, W.; Chen, T.; Chen, Z.-R.; Huang, K.-W. Ethylene polymerization by PN_3-type pincer chromium(III) complexes. *J. Mol. Catal. A: Chem.* **2014**, *395*, 100−107.
(51) Alzamly, A.; Gambarotta, S.; Korobkov, I. Synthesis, structures, and ethylene oligomerization activity of bis(phosphanylamine) pyridine chromium/aluminate complexes. *Organometallics* **2013**, *32*, 7107−7115.
(52) Mastalir, M.; De Aguiar, S. R.; Glatz, M.; Stöger, B.; Kirchner, K. A Convenient solvothermal synthesis of group 6 PNP pincer tricarbonyl complexes. *Organometallics* **2016**, *35*, 229−232.
(53) Fryzuk, M. D.; Leznoff, D. B.; Rettig, S. J. Synthesis and structure of a five-coordinate organochromium(III) thiolate complex from a chromium(II) alkyl precursor. *Organometallics* **1997**, *16*, 5116−5119.
(54) Fryzuk, M. D.; Leznoff, D. B.; Rettig, S. J.; Young Jr, V. G. One-electron oxidation of Paramagnetic chromium(II) alkyl complexes with alkyl halides: synthesis and structure of five-coordinate chromium(III) complexes. *J. Chem. Soc., Dalton Trans.* **1999**, 147−154.
(55) Simler, T.; Braunstein, P.; Danopoulos, A. A. Chromium(II) pincer complexes with dearomatized PNP and PNC ligands: a comparative study of their catalytic ethylene oligomerization activity. *Organometallics* **2016**, *35*, 4044−4049.
(56) Kallmeier, F.; Fertig, R.; Irrgang, T.; Kempe, R. Chromium-catalyzed alkylation of amines by alcohols. *Angew. Chem., Int. Ed.* **2020**, *59*, 11789−11793.
(57) Ott, J. C.; Isak, D.; Melder, J. J.; Wadepohl, H.; Gade, L. H. Single or paired? Structure and reactivity of PNP-Chromium(II) hydrides. *Inorg. Chem.* **2020**, *59*, 14526−14535.
(58) Prokopchuk, D. E.; Morris, R. H. Inner-sphere activation, outer-sphere catalysis: theoretical study on the mechanism of transfer hydrogenation of ketones using iron(II) PNNP eneamido complexes. *Organometallics* **2012**, *31*, 7375−7385.
(59) Demmans, K. Z.; Olson, M. E.; Morris, R. H. Asymmetric transfer hydrogenation of ketones with well-defined manganese(I) PNN and PNNP complexes. *Organometallics* **2018**, *37*, 4608−4618.
(60) Sui-Seng, C.; Freutel, F.; Lough, A. J.; Morris, R. H. Highly efficient catalyst systems using iron complexes with a tetradentate PNNP ligand for the asymmetric hydrogenation of polar bonds. *Angew. Chem., Int. Ed.* **2008**, *47*, 940−943.
(61) Lagaditis, P. O.; Lough, A. J.; Morris, R. H. Low-valent eneamido iron complexes for the asymmetric transfer hydrogenation of acetophenone without base. *J. Am. Chem. Soc.* **2011**, *133*, 9662−9665.
(62) Mikhailine, A. A.; Maishan, M. I.; Morris, R. H. Asymmetric transfer hydrogenation of ketimines using well-defined iron(II)-based precatalysts containing a PNNP ligand. *Org. Lett.* **2012**, *14*, 4638−4641.
(63) Sues, P. E.; Lough, A. J.; Morris, R. H. Stereoelectronic factors in iron catalysis: synthesis and characterization of aryl-substituted iron(II) carbonyl P-N-N-P complexes and their use in the asymmetric transfer hydrogenation of ketones. *Organometallics* **2011**, *30*, 4418−4431.
(64) Prokopchuk, D. E.; Sonnenberg, J. F.; Meyer, N.; Zimmer-De Iuliis, M.; Lough, A. J.; Morris, R. H. A spectroscopic and DFT study of ferraaziridine complexes formed in the transfer hydrogenation of acetophenone catalyzed using trans-$[Fe(CO)(NCMe)(PPh_2C_6H_4CH=NCH_2\text{-})_2\text{-}\kappa^4_{P,N,N,P}](BF_4)_2$. *Organometallics* **2012**, *31*, 3056−3064.
(65) Mikhailine, A. A.; Morris, R. H. Effect of the structure of the diamine backbone of P- N- N- P ligands in iron(II) complexes on catalytic activity in the transfer hydrogenation of acetophenone. *Inorg. Chem.* **2010**, *49*, 11039−11044.
(66) Zuo, W.; Lough, A. J.; Li, Y. F.; Morris, R. H. Amine (imine) diphosphine iron catalysts for asymmetric transfer hydrogenation of ketones and imines. *Science* **2013**, *342*, 1080−1083.
(67) Lagaditis, P. O.; Mikhailine, A. A.; Lough, A. J.; Morris, R. H. Template synthesis of iron(II) complexes containing tridentate P-N-S, P-N-P, P-N-N, and tetradentate P-N-N-P ligands. *Inorg. Chem.* **2010**, *49*, 1094−1102.
(68) Ajayi, T. J.; Shapi, M. Solvent-free mechanochemical synthesis, Hirshfeld surface analysis, crystal structure, spectroscopic characterization and NBO analysis of bis (ammonium) bis ((4-methoxyphenyl) phosphonodithioato)-nickel(II) dihydrate with DFT studies. *J. Mol. Struct.* **2020**, *1202*, 127254.
(69) Ajayi, T. J.; Pillay, M. N.; van Zyl, W. E. Solvent-free mechanochemical synthesis of dithiophosphonic acids and corre-

https://doi.org/10.1021/acsomega.4c02076
ACS Omega 2024, 9, 19690−19699

sponding nickel(II) complexes. *Phosphorus, Sulfur Silicon Relat. Elem.* **2017**, *192*, 1205−1211.
(70) Maser, L.; Vogt, M.; Langer, R. Facial vs. meridional coordination modes in Re^{I} tricarbonyl complexes with a carbodiphosphorane-based tridentate ligand. *Anorg. Allg. Chem.* **2021**, *647*, 1518−1523.
(71) Tamayo, A. B.; Alleyne, B. D.; Djurovich, P. I.; Lamansky, S.; Tsyba, I.; Ho, N. N.; Bau, R.; Thompson, M. E. Synthesis and characterization of facial and meridional tris-cyclometalated iridium-(III) complexes. *J. Am. Chem. Soc.* **2003**, *125*, 7377−7387.
(72) McDaniel, A. M.; Tseng, H.-W.; Damrauer, N. H.; Shores, M. P. Synthesis and solution phase characterization of strongly photooxidizing heteroleptic Cr(III) tris-dipyridyl complexes. *Inorg. Chem.* **2010**, *49*, 7981−7991.
(73) Lever, A. P. *Inorganic Electronic Spectroscopy*; Elsevier Publishing Company: Amsterdam, The Netherlands, 1984; Vol. *33*.
(74) Moulin, J. O.; Evans, J.; McGuinness, D. S.; Reid, G.; Rucklidge, A. J.; Tooze, R. P.; Tromp, M. Probing the effects of ligand structure on activity and selectivity of Cr(III) complexes for ethylene oligomerisation and polymerisation. *Dalton Trans.* **2008**, 1177−1185.
(75) Figgis, B. *Introduction to Ligand Fields"*; Interscience Publ: New York, USA, 1966; Vol. *5*.
(76) Sinha, N.; Yaltseva, P.; Wenger, O. S. The nephelauxetic effect becomes an important design factor for photoactive first-Row transition metal complexes. *Angew. Chem., Int. Ed.* **2023**, *62*, No. e202303864.
(77) Sharma, A. K.; Chandra, S. Complexation of nitrogen and sulphur donor Schiff's base ligand to Cr(III) and Ni(II) metal ions: synthesis, spectroscopic and antipathogenic studies. *Spectrochim. Acta A Mol.* **2011**, *78*, 337−342.
(78) Chandra, S.; Sharma, A. K. Applications of several spectral techniques to characterize coordination compounds derived from 2, 6-diacetylpyridine derivative. *Spectrochim. Acta A Mol.* **2009**, *74*, 271−276.
(79) Porterfield William, W. *Inorganic Chemistry, A Unified Approach*; Addison Wesley Pub. Co: Indiana, USA, 1984.
(80) De Buysser, K.; Herman, G.; Bruneel, E.; Hoste, S.; Van Driessche, I. Determination of the number of unpaired electrons in metal-complexes. A comparison between the Evans' method and susceptometer results. *J. Chem. Phys.* **2005**, *315*, 286−292.
(81) Su, J.; Duan, L.; Zheng, W. Chromium(III) complexes with 1, 2, 4-diazaphospholide and 2, 6-bis (N-1, 2, 4-diazaphosphol-1-yl) pyridine ligands: synthesis, X-ray structural characterization, EPR spectroscopy analysis, and magnetic susceptibility studies. *Z. Naturforsch. B Chem. Sci.* **2016**, *71*, 795−802.
(82) Gabriel, C.; Raptopoulou, C. P.; Terzis, A.; Lalioti, N.; Salifoglou, A. Synthesis, structural, spectroscopic and magnetic susceptibility studies of a soluble Cr(III)-heida (2-hydroxyethyliminodiacetic acid) complex. Relevance to aqueous chromium(III)-heida speciation. *Inorg. Chim. Acta* **2007**, *360*, 513−522.
(83) Clément, N.; Toussaint, C.; Rogez, G.; Loose, C.; Kortus, J.; Brelot, L.; Choua, S.; Dagorne, S.; Turek, P.; Welter, R. Novel Cr^{III} dinuclear complexes supported by salicyloylhydrazono dithiolane and dithiane ligands: synthesis, stability, crystal structures and magnetic properties. *Dalton Trans.* **2010**, *39*, 4579−4585.
(84) Kim, D.; Chang, J. Determination of stannous chloride and stannic bromide speciation in concentrated Cl^{-} and Br^{-} media by cyclic voltammetry. *J. Electroanal. Chem.* **2017**, *785*, 20−25.
(85) Murugappan, K.; Arrigan, D. W.; Silvester, D. S. Electrochemical behavior of chlorine on platinum microdisk and screen-printed electrodes in a room temperature ionic liquid. *J. Phys. Chem. C* **2015**, *119*, 23572−23579.
(86) Popov, I. A.; Mehio, N.; Chu, T.; Davis, B. L.; Mukundan, R.; Yang, P.; Batista, E. R. Impact of ligand substitutions on multielectron redox properties of Fe complexes supported by nitrogenous chelates. *ACS Omega* **2018**, *3*, 14766−14778.
(87) King, A. P.; Gellineau, H. A.; MacMillan, S. N.; Wilson, J. J. Physical properties, ligand substitution reactions, and biological activity of Co(III)-Schiff base complexes. *Dalton Trans.* **2019**, *48*, 5987−6002.
(88) Schnider, P.; Koch, G.; Prétôt, R.; Wang, G.; Bohnen, F. M.; Krüger, C.; Pfaltz, A. Enantioselective hydrogenation of imines with chiral (phosphanodihydrooxazole) iridium catalysts. *Chem.—Eur. J.* **1997**, *3*, 887−892.
(89) Aranda, B.; Valdebenito, G.; Parra-Melipán, S.; López, V.; Moya, S.; Vega, A.; Aguirre, P. Hydrogenation of imines catalyzed by ruthenium(II) complexes containing phosphorus-nitrogen ligands via hydrogen transfer reaction. *Mol. Catal.* **2022**, *526*, 112374.
(90) Bagh, B.; Stephan, D. W. Half sandwich ruthenium(II) hydrides: hydrogenation of terminal, internal, cyclic and functionalized olefins. *Dalton Trans.* **2014**, *43*, 15638−15645.
(91) Ling, L.; Hu, C.; Long, L.; Zhang, X.; Zhao, L.; Liu, L. L.; Chen, H.; Luo, M.; Zeng, X. chromium-catalyzed stereodivergent E- and Z-selective alkyne hydrogenation controlled by cyclic (alkyl)-(amino) carbene ligands. *Nat. Commun.* **2023**, *14*, 990.
(92) Kariofillis, S. K.; Doyle, A. G. Synthetic and mechanistic implications of chlorine photoelimination in nickel/photoredox C(sp(3))-H cross-coupling. *Acc. Chem. Res.* **2021**, *54*, 988−1000.

https://doi.org/10.1021/acsomega.4c02076
ACS Omega 2024, 9, 19690−19699